Study on Optical and Structural Properties of TiO_2/SnO_2 Thin Film for Optical Devices

Ved Prakash Meena[1,a], S S Sharma[2,b], M K Jangid[1,c]

[1] *Department of Physics, Vivekananda Global University, Jaipur, Rajasthan-303012, India.*
[2] *Department of Physics (H & S), Govt. Mahila Engineering College, Ajmer, Rajasthan-305002, India*

[a] vedprakash1581997@gmail.com
[b] shyam@gweca.ac.in
[c] mahesh.jangid@vgu.ac.in

Abstract

The TiO_2/SnO_2 thin films have garnered considerable attention for their application in optical devices due to their superior transparency and stability. This study investigates the optical and structural properties of TiO_2/SnO_2 thin films prepared through electron beam (e-beam) evaporation. The films were annealed at 400 °C for one hour in a muffle furnace to evaluate the influence of annealing on their properties. Characterization techniques, including X-ray diffraction (XRD), UV-Vis spectroscopy, and atomic force microscopy (AFM), were employed to analyze the films. XRD analysis confirmed the presence of a distinct anatase TiO_2 phase with SnO_2 inclusions. Post-annealing, an enhancement in the peak intensities of both phases was observed, signifying improved crystallinity and atomic ordering. UV-Vis spectroscopy revealed that the annealed films exhibited reduced optical absorbance compared to their pristine counterparts. Furthermore, the optical bandgap increased from 4.10 eV for the pristine films to 4.32 eV after annealing. In AFM analysis 2D and 3D surface topographical images demonstrated that the annealed films show a smoother surface with reduced roughness, attributed to the enhanced crystallinity, which mitigates structural defects and grain boundary irregularities. These findings highlight the exceptional optical and structural characteristics of TiO_2/SnO_2 thin films, suggesting their potential for use in antireflective coatings, photodetectors, and waveguide structures in optoelectronic devices.

Keywords: Thin film; E-Beam; XRD; UV-Vis; AFM.
Received 27 January 2025; First Review 22 February 2025; Accepted 22 February 2025

*** Address of correspondence**
Ved Prakash Meena
Department of Physics, Vivekananda Global University, Jaipur, Rajasthan-303012, India.

Email: vedprakash1581997@gmail.com

How to cite this article
Ved Prakash Meena, S S Sharma, M K Jangid, Study on Optical and Structural Properties of TiO_2/SnO_2 Thin Film for Optical Devices, J. Cond. Matt. 2024; 02 (02): 81-85.

Available from:
https://doi.org/10.61343/jcm.v2i02.65

Introduction

Titanium dioxide (TiO_2) stands out as one of the most extensively utilized semiconductors due to its numerous advantageous physicochemical properties. These include its abundance, affordability, biocompatibility, chemical stability, and resistance to corrosion [1]. As a result, TiO_2 finds application in diverse fields. However, a major limitation of TiO_2 as a photocatalyst is its high electron-hole recombination rate, which reduces its efficiency [2-3]. To address this, coupling TiO_2 with other semiconductors has proven to be an effective strategy. Tin oxide (SnO_2), despite its wide band gap of 3.8 eV, has been successfully employed in combination with TiO_2. This can be achieved either by doping TiO_2 with tin ions or by creating TiO_2-SnO_2 composites [4-7]. The development of advanced materials for optical devices has been a key factor driving technological progress in modern optoelectronics. Because of their remarkable optical transparency, stability, and adjustable qualities, thin films based on titanium dioxide (TiO_2) and tin dioxide (SnO_2) have become attractive options among these materials. Particularly, the TiO_2/SnO_2 thin films have earned interest due to its possible uses in waveguide structures, photodetectors, and antireflective coatings, among other optical devices. These uses make use of the distinct optical and structural properties of SnO_2 and TiO_2, which can be further improved by post-deposition treatments and material engineering [8-9]. A well-known substance, titanium dioxide has a broad bandgap, robust photocatalytic activity, and good optical transmittance in the visible spectrum [10-11]. Applications needing high transparency and low absorption losses commonly use it [12]. Tin dioxide, a semiconductor with a wide bandgap of 3.6 eV, is also a perfect complimentary material for creating composite thin films because of its strong chemical stability, high electrical conductivity, and optical

transparency [13-14]. It has been demonstrated that combining TiO_2 and SnO_2 into a thin-film system improves overall material stability, decreases optical losses, and strengthens light-matter interactions [15]. Researchers have synthesized TiO_2/SnO_2 thin films using various deposition techniques, including sol-gel processing, electron-beam evaporation, and chemical vapor deposition. Optimizing the optical and structural properties of films requires precise control over their composition, thickness, and homogeneity, all of which may be achieved using electron-beam evaporation technique [16]. The annealing process is one important element affecting these thin films' performance. The heat process of annealing has a major impact on the material's defect density, grain structure, and crystallinity. By increasing their crystallinity and decreasing defects, annealing TiO_2/SnO_2 films at optimal temperatures enhances their optical characteristics, including transparency and bandgap tunability [17]. According to recent studies, annealing can result in a small shift in the optical bandgap and a decrease in visible spectrum absorption, both of which are signs of enhanced material quality [18-19]. The TiO_2/SnO_2 thin films' structural characteristics are also crucial in evaluating whether or not they are appropriate for use in optical devices. The existence of SnO_2 inclusions, which further enhance the structural stability and performance of the film, and the anatase phase of TiO_2, which is linked to enhance optical and photocatalytic capabilities, have been discovered by X-ray diffraction (XRD) investigations. The film's functionality in optoelectronic devices is improved by annealing, which refines grain boundaries and reduces imperfections, boosting the film's ability to propagate light efficiently [20-21]. This research seeks to thoroughly explore the impact of the annealing process on the optical and structural characteristics of TiO_2/SnO_2 thin films. The results are expected to suggest valuable insights for enhancing the performance of TiO_2/SnO_2 thin films in various optoelectronic devices.

Experimental

TiO_2/SnO_2 thin films with a thickness of 300 nm were deposited onto glass substrates through the electron-beam deposition method. High-purity titanium dioxide (TiO_2, 99.99%) and tin dioxide (SnO_2, 99.98%) were employed as source materials for film preparation. Equal weight ratios of these oxides were thoroughly blended using high-energy planetary ball milling to ensure uniform mixing. The milling process was carried out for 5 hours, resulting in a homogenous powder mixture. This powder was then dried and compressed into pellets under a biaxial pressure of 10 tons. The thin films were deposited using an e-beam deposition system (Model BC-300 HHV). A vacuum chamber was utilized, which was evacuated to a base pressure of approximately 10^{-5} mbar with the help of rotary and diffusion pumps. The substrate temperature remained at room temperature throughout the process. The target to substrate distance was fixed at 35 cm. To study the effect of annealing temperature, the prepared samples were annealed at 400 °C for one hour in a muffle furnace. For structural characterization, X-ray diffraction (XRD) was performed at room temperature using a Panalytical X'Pert Pro diffractometer with CuKα radiation (λ = 0.15406 nm) to determine the phases present. The optical properties of the thin films were examined using UV-Vis absorption spectroscopy (Shimadzu UV-1800) across a wavelength range of 200-800 nm. Surface topography was analyzed using Atomic Force Microscopy (AFM). Both 2D and 3D images of the thin films were obtained with a Bruker Multimode Scanning Probe.

Results and Discussion

XRD analysis

Figure 1 shows the X-ray diffraction patterns of pristine and annealed TiO_2/SnO_2 thin films. In the TiO_2/SnO_2 samples, distinct peaks corresponding to TiO_2 were observed at 2θ = 25.47°, 38.19°, and 78.97°, which are indexed to the (101), (004), and (224) planes of anatase-phase TiO_2 (JCPDS No. 21-1272). These peaks indicate that the anatase phase is the predominant crystalline structure in the film, demonstrating strong crystallinity, consistent with earlier reports on TiO_2 thin films [22-23]. For SnO_2, diffraction peaks were identified at 2θ = 51.97°, 58.05°, 66.24°, and 71.51°, corresponding to the (221), (310), (301), and (220) planes of rutile-phase SnO_2 (JCPDS No. 41-1445). These peaks confirm the polycrystalline nature of SnO_2 and validate its successful incorporation into the composite thin film, aligning with findings from previous studies [24-25]. After annealing, an improvement in the peak intensities of both TiO_2 and SnO_2 was observed, indicating enhanced crystallinity and better atomic ordering within the thin films. The annealing effects have been broadly reported to facilitate the reorganization of atoms and reduction of structural defects in thin films, leading to sharper and more intense diffraction peaks. This effect is particularly prominent in mixed oxide systems like TiO_2/SnO_2, where thermal treatment promotes the growth of crystalline domains and strengthens the diffraction signals associated with the respective phases. Furthermore, annealing may also influence the redistribution of oxygen vacancies and stoichiometric balance in the film, additional contributing to the improved peak intensity. Such enhancements are consistent with studies where annealing has been shown to significantly improve the structural properties and crystallinity of oxide thin films [26-27]. The properties and applications of thin films are highly influenced by their structural parameters. To analyze these parameters, the

crystallite size (D), microstrain (ε), and dislocation density (δ) can be determined using the following equations:

The crystallite size (D) can be estimated from the peaks of the XRD diffractogram using Scherrer's formula [28]:

$$D = \frac{K\lambda}{\beta\cos\theta} \qquad (1)$$

The dislocation density (δ), which represents the length of dislocation lines per unit volume ($Å^{-2}$) of the crystal, was calculated using the formula [29]:

$$\delta = \frac{1}{D^2} \qquad (2)$$

The lattice strain (ε) is derived from Scherrer's relation [30]:

$$\varepsilon = \frac{\beta}{4\tan\theta} \qquad (3)$$

Here, K is a geometrical factor with a value of 0.9, λ=1.5406 A˚ is the X-ray wavelength (Cu Kα radiation, equivalent to 0.154 nm), β is the full width at half maximum (FWHM) of the primary diffraction peaks, and θ is the Bragg diffraction angle.

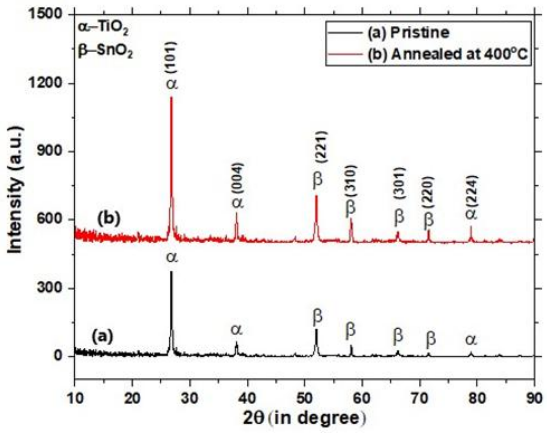

Figure 1: XRD pattern of (a) pristine and (b) annealed TiO_2/SnO_2 thin films

Table 1: Structural parameters of TiO_2/SnO_2 thin films

Sample	2θ	β	D (Å)	ε (×10^{-3})	δ (10^{16}/ m^2)
Pristine	25.47	0.236	6.02	260.77	275.94
Annealed at 400 ˚C	25.47	0.117	12.15	129.28	67.74

Table 1 provides the structural parameters of TiO_2/SnO_2 thin films, highlighting the effects of annealing at 400 °C. The diffraction angle (2θ) remains unchanged at 25.47° for both pristine and annealed samples. However, annealing reduces the Full Width at Half Maximum (FWHM) from 0.236 to 0.117, indicating a growth in crystallite size (D) from 6.02 Å to 12.15 Å. This signifies improved crystal quality. Simultaneously, lattice strain (ε) decreases from 260.77 × 10^{-3} to 129.28 × 10^{-3}, and dislocation density (δ) drops from 275.94 × 10^{16}/m² to 67.74 × 10^{16}/m², reflecting reduced structural defects post-annealing.

Optical Properties

Figure 3 presents the optical absorption spectra of TiO_2/SnO_2 thin films, highlighting the distinct differences in absorption between pristine and annealed samples. The data reveal that the annealed TiO_2/SnO_2 films exhibit lower optical absorbance compared to their pristine counterparts. This reduction in absorbance upon annealing is associated with modifications in structural and optical properties. Annealing is essential for enhancing the crystallinity of thin films. It helps minimize defects, including dislocations and grain boundaries. This often act as scattering centers for light. As a result, annealed TiO_2/SnO_2 thin films show enhanced optical transmittance, enabling more efficient light penetration through the material [31]. Furthermore, the annealing process contributes to better alignment of the film's crystal structure, thereby facilitating improved light-harvesting capabilities by minimizing non-radiative recombination of charge carriers [32]. These properties make annealed TiO_2/SnO_2 thin films more suitable for applications in optoelectronics, photovoltaics, and photocatalysis [33-34].

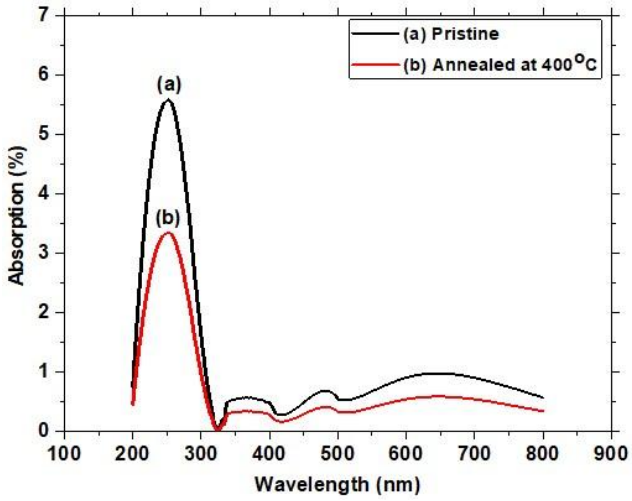

Figure 2: Absorption spectra of (a) pristine and (b) annealed TiO_2/SnO_2 thin films

The bandgap energy for the films was determined using the Tauc relation [35], which is expressed as:

$$\alpha h\nu = A(h\nu - E_g)^m \qquad (4)$$

where h is Planck's constant, ν is the photon frequency, α is the absorption coefficient derived from the absorbance data, E_g is the bandgap energy, and m is the power factor of the transition mode. For direct transitions, m equals 0.5 was used to calculate the bandgap.

The study reveals a notable increase in the optical bandgap of TiO_2/SnO_2 thin films upon annealing, shifting from 4.10 eV for the pristine films to 4.32 eV for the annealed ones. This bandgap widening is closely linked to the annealing process, which improves the crystallinity of the films and reduces the density of localized states at grain boundaries [36-37].

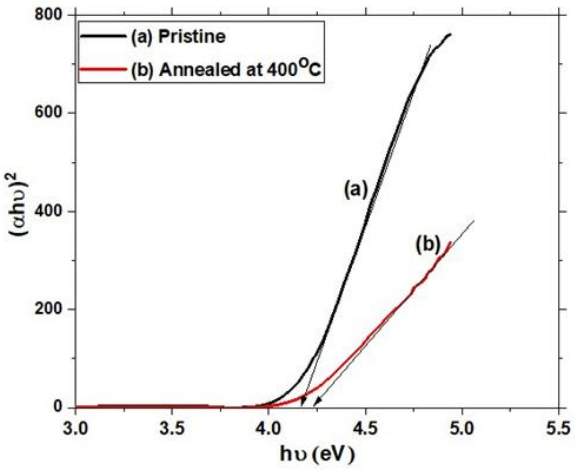

Figure 3: Tauc plots of (a) pristine and (b) annealed TiO_2/SnO_2 thin films

These localized states, typically caused by structural imperfections, contribute to sub-bandgap energy levels that facilitate undesired light absorption. By minimizing these defects, annealing effectively sharpens the band edge, resulting in a higher optical bandgap. The increased bandgap and refined absorption properties make annealed TiO_2/SnO_2 films highly suitable for applications requiring wide-bandgap materials. For instance, they hold promise as efficient UV photodetectors due to their selective sensitivity to ultraviolet light while maintaining transparency in the visible spectrum. They also show promise as transparent conducting oxides (TCOs). This makes them suitable for applications in optoelectronic devices. TCOs require high optical transparency and conductivity, both of which are enhanced by the annealing-induced structural improvements in TiO_2/SnO_2 films [38-39].

AFM Analysis

AFM is a vital way for investigating the surface topography of thin films with nanometer-scale resolution, offering insights into the structural and functional properties of the materials. Figure 4 depicts the AFM images of TiO_2/SnO_2 thin films in their (a) pristine and (b) annealed states. The analysis reveals that both films exhibit a granular and uniform surface morphology, indicative of densely packed nanostructures [40-41].

Upon annealing, significant changes in the surface properties are observed. The annealed TiO_2/SnO_2 thin films display a smoother surface with reduced roughness compared to the pristine films. This reduction in surface roughness is attributed to the enhanced crystallinity induced by annealing, which minimizes structural defects and grain boundary irregularities. Such improvements in surface uniformity are crucial for optimizing the optical and electronic performance of the films [42]. The densely packed nanostructures observed in the AFM images contribute to the films' optical clarity and efficient light management, essential for applications in optoelectronic devices. Furthermore, the smoother and more uniform surface after annealing enhances film stability and charge transport, making these films promising candidates for use in high-performance photovoltaics, UV photodetectors, and transparent conductive oxides [43].

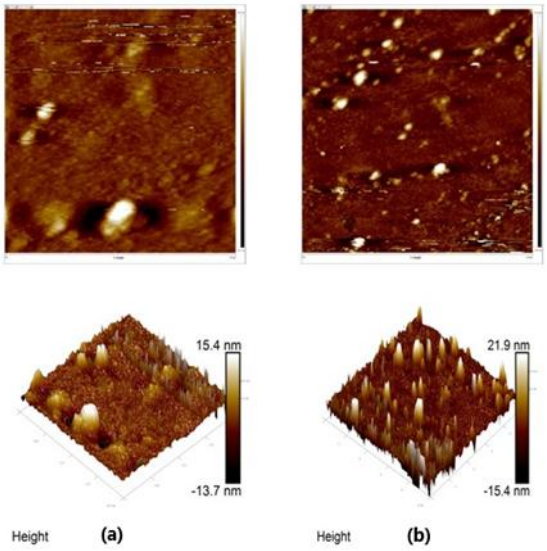

Figure 4: AFM 2D and 3D images of (a) pristine and (b) annealed TiO_2/SnO_2 thin films

Conclusion

The study of TiO_2/SnO_2 thin films provides valuable insights into the impact of annealing temperature on their structural and optical characteristics. Post-annealing XRD patterns indicate stability in the crystalline structure, suggesting minimal introduction of stress or defects during the process. Notably, annealing at 400 °C results in significant bandgap enhancement, increasing from 4.15 eV to 4.34 eV. This improvement is attributed to enhanced crystallinity, reduced defects such as oxygen vacancies, and improved interfacial properties. These modifications are crucial for optimizing the functionality of TiO_2/SnO_2 thin films in applications such as UV detectors, transparent conductive oxides, and photocatalysis. Furthermore, AFM analysis reveals that annealing substantially affects surface morphology. The annealed TiO_2/SnO_2 thin films show a smoother surface with reduced roughness compared to the pristine films. This study emphasizes the essential role of annealing temperature in fine-tuning the properties of TiO_2/SnO_2 thin films, identifying 400 °C as the optimal

temperature for achieving superior performance in advanced technological applications.

Acknowledgements

The authors (Specially Ved Prakash Meena) are highly thankful to UGC for providing financial support under JRF scheme to carry out this work. They also express their gratitude to the Material Science Laboratory developed at Government Mahila Engineering College, Ajmer under TEQIP-II and Material Research Centre, MNIT Jaipur (India) for providing experimental and measurement facilities.

References

1. J Coronado, F Fresno, M Hernández-Alonso, R Portela, S Suárez, S García Rodríguez, and V de la Peña O'Shea. Design of Advanced Photocatalytic Materials for Energy and Environmental Applications. 2013.
2. M R D Khaki, M S Shafeeyan, A A A Raman, and W M A W Daud. J. Environ. Manag., 198:78–94, 2017.
3. V Kumaravel, S Mathew, J Bartlett, and S C Pillai. Appl. Catal. B Environ., 244:1021–1064, 2019.
4. H Tada, A Hattori, Y Tokihisa, K Imai, N Tohge, and S Ito. J. Phys. Chem. B, 104:4585–4587, 2000.
5. K Awa, R Akashi, A Akita, S ichi Naya, H Kobayashi, and H Tada. Chem. Phys. Chem., 20:2155–2161, 2019.
6. W Sangchay. Energy Procedia, 89:170–176, 2016.
7. A Kusior, L Zych, K Zakrzewska, and M Radecka. Appl. Surf. Sci., 471:973–985, 2019.
8. M Gülkı, Y Yılmaz, and T Aydogan. Appl. Surf. Sci., 554:149610, 2021.
9. M K Jangid, S Sharma, V P Meena, V P Arya, and S S Sharma. Evergreen, 11:178-185, 2024.
10. L Zhang, Y Wang, and H Zhao. Mater. Today Chem., 17:100303, 2020.
11. M K Jangid, S P Nehra, and M Singh. AIP Conf. Proc., 1393:311-312, 2011.
12. A Fujishima, K Honda, and S Kikuchi. Nature, 238:37–38, 1972.
13. C G Granqvist. Sol. Energy Mater. Sol. Cells, 91:1529–1598, 2007.
14. M K Jangid and M Singh. Int. J. Phys. Res., 2:15-23, 2012.
15. T Wågberg, P Johansson, and E Lindahl. Thin Solid Films, 539:114–121, 2013.
16. R Jafari, S Davari, and M Amjadi. J. Phys. D: Appl. Phys., 48:085303, 2015.
17. S Kumar, V Sharma, and P Singh. J. Mater. Sci.: Mater. Electron., 30:1675–1684, 2019.
18. J Lee, Y Kim, and H Park. ACS Appl. Mater. Interfaces, 10:175–185, 2018.
19. M K Jangid, S S Sharma, J Ray, D K Yadav, and C Lal. Int. J. Hydrogen Energy, 48:37921-37929, 2023.
20. P S Reddy, R Sharma, and K Ghosh. Ceram. Int., 46:16014–16021, 2020.
21. M K Jangid, S P Nehra, and M Singh. AIP Conf. Proc., 1349:685-686, 2011.
22. X Liu, J Wang, and L Chen. J. Mater. Sci., 42:640–645, 2007.
23. S Kumar, R Patel, and A Gupta. Thin Solid Films, 518:2795–2799, 2010.
24. F A Deorsola and D Vallauri. J. Mater. Sci., 43:3274–3278, 2008.
25. M M Miah, T Ahmed, and N Akhtar. J. Appl. Phys., 110:093510, 2011.
26. M Gharbi, R Karoui, and S Azzouz. J. Mater. Sci., 44:4312–4319, 2009.
27. S Shokri and M Parvin. Thin Solid Films, 520:5850–5854, 2012.
28. C Messaadi, T Ghrib, and J Jalali. J. Curr. Nanosci., 15:398–406, 2019.
29. G B Williamson and R C Smallman. Philos. Mag., 1:34–45, 1956.
30. B D Cullity. Elements of X-ray Diffraction. Addison-Wesley, London, 1978.
31. S Sakka. J. Non-Cryst. Solids, 100:227–239, 1988.
32. M K Jangid, S P Nehra, and M Singh. J. Nano-Electron. Phys., 3:460-468, 2011.
33. L Zhang, Y Li, and T Xu. J. Mater. Sci., 2021.
34. P Singh, A Mehta, and K Verma. Adv. Opt. Mater., 2020.
35. J Tauc. Mater. Res. Bull., 3:37–46, 1968.
36. A Fujishima and K Honda. Nature, 238:37–38, 1972.
37. M K Jangid, S S Sharma, J Ray, and S Jangid. Mater. Today: Proc., 67:847-851, 2022.
38. S Kumar, R Sharma, and M Gupta. J. Appl. Phys., 2022.
39. L Wang, H Zhang, and J Liu. Adv. Funct. Mater., 2021.
40. P Patra, S Mishra, and K Verma. Prog. Mater. Sci., 135:101073, 2023.
41. M K Jangid and S K Jangid. Trends Sci., 19:2067, 2022.
42. P Singh, A Sharma, and R Verma. J. Surf. Sci. Eng., 2021.
43. L Zhang, T Li, and H Xu. Adv. Thin Film Mater., 2022.